Short-lived Alpha Power Suppression Induced by Low-intensity Arrhythmic rTMS

Elina Zmeykina, [a] **Matthias Mittner,** [b] **Walter Paulus** [a] **and Zsolt Turi** [a,c*]

[a] *Department of Clinical Neurophysiology, University Medical Center Göttingen, Germany*

[b] *Department of Psychology, UiT The Arctic University of Norway, Norway*

[c] *Department of Neuroanatomy, Institute of Anatomy and Cell Biology, University of Freiburg, Germany*

Abstract—**This study was conducted to provide a better understanding of the role of electric field strength in the production of aftereffects in resting state scalp electroencephalography by repetitive transcranial magnetic stimulation (rTMS) in humans. We conducted two separate experiments in which we applied rTMS over the left parietal-occipital region. Prospective electric field simulation guided the choice of the individual stimulation intensities. In the main experiment, 16 participants received rhythmic and arrhythmic rTMS bursts at between ca. 20 and 50 $^{mV}/_{mm}$ peak absolute electric field intensities. In the control experiment, another group of 16 participants received sham rTMS. To characterize the aftereffects, we estimated the alpha power (8–14 Hz) changes recorded in the inter-burst intervals, i.e., from 0.2 to 10 s after rTMS. We found aftereffects lasting up to two seconds after stimulation with ca. 35 $^{mV}/_{mm}$. Relative to baseline, alpha power was significantly reduced by the arrhythmic protocol, while there was no significant change with the rhythmic protocol. We found no significant long-term, i.e., up to 10-second, differences between the rhythmic and arrhythmic stimulation, or between the rhythmic and sham protocols. Weak arrhythmic rTMS induced short-lived alpha suppression during the inter-burst intervals. © 2021 IBRO. Published by Elsevier Ltd. All rights reserved.**

Key words: repetitive transcranial magnetic stimulation, electroencephalography, alpha power, aftereffect, individual alpha frequency, electric field.

INTRODUCTION

The self-organized activity of neurons and neural assemblies produces oscillating electric fields in the brain (Anastassiou et al., 2011). These oscillating electric fields are recurrent, as they feed back onto the neural assemblies thereby facilitating neural synchrony and plasticity (Anastassiou et al., 2011). Repetitive transcranial magnetic stimulation (rTMS) induces a periodic electromagnetic field in the brain (Paulus et al., 2013), which triggers molecular, cellular, and electrophysiological changes in neuro-glia networks (Lenz & Vlachos, 2016).

In our previous work, we studied the immediate electrophysiological effects of rTMS using a novel stimulation intensity selection approach (Zmeykina et al., 2020). In order to individually adapt the stimulation intensities, we prospectively estimated the rTMS-induced electric field strengths (Zmeykina et al., 2020). Using this approach we have shown that peak absolute electric fields between ca. 35 and 50 $^{mV}/_{mm}$ already induced

immediate changes in the electroencephalogram (EEG) in humans (Zmeykina et al., 2020).

Yet, many applications of rTMS aim at inducing neural effects that outlast the duration of the stimulation itself. Therefore, in the present study we investigated possible aftereffects of the stimulation by focusing on the EEG recordings in the inter-burst intervals from 0.2 to 10 s after the rTMS bursts. The selected time window is free from rTMS-induced artifacts such as ringing, decay, cranial muscular, somatosensory or auditory artifacts (Ilmoniemi et al., 2015).

In the present study, we focused on alpha-band frequency estimated from parietal-occipital sources, because it has high signal to noise ratio in resting state condition and posterior alpha peak frequency has a good intra-subject variability (Haegens et al., 2014). To induce electrophysiological effects, we applied rTMS at individual alpha frequencies. We estimated the spectral power in the alpha frequency band to quantify the modulation of alpha rhythm at the stimulation frequency by rTMS.

Based on the *entrainment echo* hypothesis (Hanslmayr et al., 2014), we expected that rhythmic rTMS at the individual alpha frequencies would entrain neural

*Correspondence to: Department of Neuroanatomy, Institute of Anatomy and Cell Biology, University of Freiburg, Germany (Z. Turi).
E-mail address: zsolt.turi@anat.uni-freiburg.de (Z. Turi).

oscillations and increase alpha power due to increased synchrony to the external rTMS-induced electric field. We also hypothesized that rhythmic rTMS would facilitate spike-timing dependent plasticity and thus increase alpha power up to several seconds after the stimulation cessation. On the other hand, we expected that arrhythmic (active control) or sham (90° tilt) protocols would not entrain ongoing posterior alpha oscillation and, therefore, would not produce any aftereffects.

EXPERIMENTAL PROCEDURES

Secondary analysis

To test our hypotheses we performed a secondary analysis of our openly available rTMS-EEG dataset (https://github.com/ZsoltTuri/2019_rTMS-EEG). We reported the immediate electrophysiological effects elsewhere (Zmeykina et al., 2020). This dataset contains EEG recordings from two separate experiments (see point Experimental procedure and stimulation parameters for more details).

Participants

We included only neurologically healthy participants in the study (Zmeykina et al., 2020). For more details, see Table 1.

Ethics

The Ethics Committee of the University Medical Center Göttingen approved the investigation, the experimental protocols, and all methods used in the main and control experiment (application number: 35/7/17). We performed all the experiments under the relevant guidelines and regulations. All participants gave written informed consent before participation (Zmeykina et al., 2020).

Head modeling and electric field estimation

We used a freely available open software package called Simulation of Non-invasive Brain Stimulation (SimNIBS, version 2.0.1) (Thielscher et al., 2015). We used anatomical T1- and T2-weighted and diffusion-based magnetic resonance imaging data (MRI) to generate individualized, multi-compartment head models. The head models included the following compartments (corresponding conductivity values in [S/m]): scalp (0.465), bone (0.01), cerebrospinal fluid (1.654), gray matter (0.275) and white matter (0.126). For the gray and white matter compartments, we used anisotropic conductivity values using the volume-normalized method (Opitz et al., 2011).

Experimental procedure and stimulation parameters

In the main experiment (n = 16), we performed prospective electric field modeling to individually adapt the stimulation intensities (see Fig. 1A). Participants took part in three rTMS-EEG sessions separated by at least 48 hours. In each session, we applied rTMS at 20, 35, or 50 $^{mV}/_{mm}$ peak absolute electric fields. These field values correspond to 9.5 ± 1.1%, 16.8 ± 2%, and 23.9 ± 2.5% of the group-averaged device output. We refer to these sessions as low, medium, and high intensity conditions, respectively. For further details about the rTMS protocols, see Fig. 1B (top).

In the control experiment (n = 16), an independent group of participants received sham rTMS with the coil tilted by 90° (see Fig. 1B, bottom) (Romei et al., 2012). During the measurement, this sham protocol produced acoustic and ringing/decay artifacts while it minimized the induced electric field in the brain. We used the same stimulation intensity for each participant, which we fixed at 29% of the device output. This value corresponded to the maximum pulse amplitude used in the high intensity condition of the main experiment.

In both experiments, we applied rTMS over the left parietal-occipital area, specifically at the PO3 electrode as defined by the international 10/20 EEG system. The participants received the stimulation in the resting state, eyes open condition (Fig. 1C). We delivered the rhythmic rTMS at the individual alpha frequency, which we estimated prior to each session from the resting state EEG recordings (Zmeykina et al., 2020). Based on the Arnold's tongue model of neural entrainment, this is a necessary step to maximize the efficacy of inducing neural entrainment. In the arrhythmic rTMS, we applied rTMS in a manner that avoided any rhythmicity in the timing of the consecutive pulses (Thut et al., 2011; Albouy et al., 2017). Here, we prospectively adjusted the timing of each pulse so that frequencies in the alpha frequency band (8–12 Hz) as well as their harmonics and subharmonics (e.g., 4 and 16 Hz for 8 Hz) did not occur (Zmeykina et al., 2020).

In both experiments, we used a MagPro X100 stimulator with MagOption (MagVenture, Denmark), normal coil current direction, biphasic pulses with 280 μs pulse width, and a MC-B70 figure-of-eight coil. During rTMS we simultaneously recorded the scalp EEG with a TMS-compatible, 64 channel, active EEG system (BrainProducts, Munich, Germany).

EEG analysis

EEG preprocessing. EEG analysis was performed using the FieldTrip software package (http://fieldtrip.fcdonders.

Table 1. Participant information

	Main experiment	Control experiment
Sample size (n)	16	16
Mean age ± SD (years)	25.5 ± 3.2	23.9 ± 3.9
Age range (years)	21 to 32	20 to 34
Number of women/men	8/8	8/8
Exclusion criteria assessed by	Self-reports and/or neurological examinations	
Contraindications	None	None
Mean laterality index[a] ± SD	78.4 ± 50.1	78.8 ± 31.6
Laterality index range	−30 to 100	0 to 100

[a] We assessed the handedness laterality index with the Edinburgh Handedness Inventory (Oldfield, 1971).
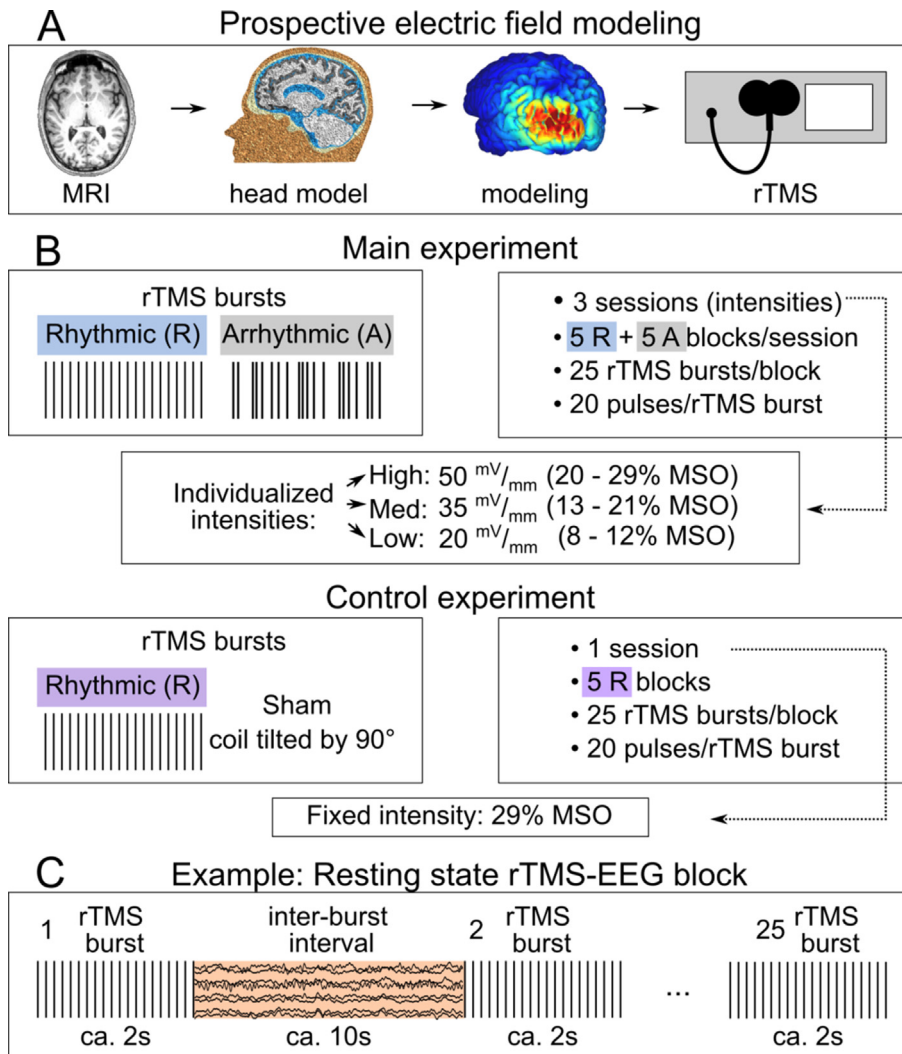
Fig. 1. Study overview. **(A)** The stimulation intensity was individually adapted based on prospective electric field modeling. **(B)** The stimulation parameters in the main and control experiments. In the control experiment, we delivered rhythmic sham rTMS. **(C)** We defined the aftereffects by focusing on the rTMS artifact-free inter-burst intervals (highlighted in orange). Abbreviations: MSO – maximum stimulator output.

50 Hz line noise. Next, the data were inspected for artifactual trials and channels. The procedure included a semi-automatic algorithm described in detail in reference (Wu et al., 2018). In brief, we defined the outlier channels and trials, which exceeded 1.5 interquartile ranges. If a trial contained fewer than 20% of such channels, they were interpolated in the trial, but otherwise removed. The channels with line noise or high impedance levels were defined by estimating the correlation coefficient with the neighboring channels. We rejected channels that had a correlation coefficient value lower than 0.4 with their neighbors. All removed channels were then interpolated using the weighted signal of the neighboring channels.

After inspecting the data we defined the number of independent components for the ICA (binICA) by estimating the eigenvalues of the covariance matrix of the EEG data. We defined the number of ICA components as the rank of the diagonal matrix minus the number of the interpolated channels. We ran ICA only on trials that did not contain any interpolated channels. Independent components were visually inspected for artifacts. The components containing eye-related artifacts, muscle, and line noise artifacts were projected out from the data. After preprocessing, 93.8 ± 9.9 (mean ± SD) trials remained for the high, 91.1 ± 13.4 trials for the medium and 92.5 ± 9.9 trials for the low intensity conditions. As the last preprocessing step, we applied two seconds of padding ('mirror') to the data intervals corresponding to baseline.

Short-term aftereffect. We performed the time–frequency analysis by running a Morlet wavelet decomposition based on multiplication in the frequency domain between 1 and 25 Hz with step 0.5 Hz. For wavelets, we used 7 cycles with the length of 3 standard deviations of the implicit Gaussian kernel. The analysis was performed for the whole length of the trial from −5.5 to 10 s around the TMS burst offset including all channels. Once the wavelet analysis was completed, we performed a statistical analysis to test the short-term aftereffect of the protocols and the time. To this aim, we used two-second intervals before ('baseline') and after ('activation') the rTMS burst. For each participant we

nl) with custom-made MATLAB code. First, the TMS-EEG data were segmented into trials that were time-locked to the offset of the rTMS burst (from 3.5 s before and 10 s after the last TMS pulse). The datasets in both experiments (main and control) included 125 trials with each stimulation condition. We removed the rTMS-induced ringing artifacts from 4 ms before to 9 ms after the TMS pulse. The first round of ICA (fastICA) was performed to automatically identify the decay artifact by averaging the time course of components over 50 ms after each TMS pulse. Components with an amplitude exceeding 30 μV were rejected. Piecewise Cubic Hermite Interpolation (pchip) replaced the time intervals around the pulses.

Then, the data were downsampled to 625 Hz. We applied a 80 Hz low-pass and a 0.1 Hz high-pass filter (Butterworth IIR filter type, 'but' in FieldTrip). A discrete Fourier transform-based filter was used to remove the

averaged the data over all trials and then performed the statistical analysis (Fieldtrip as 'actvsbslT' test) separately for each intensity condition (High, Medium, and Low). To reduce the influence of the remaining TMS artifacts we performed a cluster-based permutation test (Monte Carlo, 2–25 Hz frequency range two-tailed t-test with 1000 permutations) 0.2 s after the last TMS pulse. The null hypothesis was rejected if the p-value of the maximum cluster level statistics was below 0.05 (one-tailed test). Additionally, we performed the same statistical comparison over the seven parietal channels on the right, non-stimulated hemisphere (i.e., P2, P4, P6, P8, PO4, PO8, O2).

Long-term after effect. For the second analysis, we normalized the power of all intervals of ca. 10 s length after rTMS bursts to baseline, i.e., the 1 s period before the start of the rTMS burst, using the decibel conversion. The frequency range was normalized by extracting the IAF from the original frequency, and was averaged over IAF ± 1 Hz and over the ten left parietal channels (i.e., P7, P5, P3, P1, Pz, PO7, PO3, POz, O1, Oz). Moreover, we performed the statistical comparison specifically over the seven parietal channels on the right, non-stimulated hemisphere.

Statistical analysis of the normalized power including the selected channels and the entire trial duration from zero to ten seconds was performed for each stimulation intensity separately. First, we used the independent samples t-test to compare rhythmic real and rhythmic sham rTMS protocols in the high intensity condition. When comparing the real and sham rhythmic protocols, we focused primarily on the high intensity condition because our participants received only one sham rTMS session corresponding to the high intensity condition in the main experiment. Note that in the sham protocol we fixed the stimulation intensity at 29% of the device output. To compare the rhythmic and arrhythmic conditions we used dependent sample t-tests separately for each intensity condition at IAF ± 1 Hz. A non-parametric Monte Carlo approach with 1000 randomizations was performed to estimate the probability of whether a given amount of significant electrodes ($p < 0.05$) could be expected by chance. For effect sizes, we report Cohen's d and partial eta squared (η^2) values.

RESULTS

Short-term aftereffect

We performed all analyses on the entire sample ($n = 16$). First, we focused on analyzing the alpha power change following the rTMS bursts and compared it to the baseline value. In the rhythmic conditions, the analysis revealed no statistically significant differences from baseline in any of the intensity conditions (all p-values >0.05; see Fig. 2). In the arrhythmic condition, there was a significant decrease at medium intensity ($t_{15} = -4.01$, $p = 0.03$; Cohen's $d = 0.70$ and $\eta^2 = 0.1$). Further analysis revealed that at the individual level ten out of 16 participants showed alpha power decrease, three showed no change and three

demonstrated alpha power increase after arrhythmic rTMS. However, we found no significant aftereffects at any other intensities (all p-values > 0.05; see Fig. 2B). Lastly, the analysis revealed that the alpha power did not change significantly from baseline after the sham protocol ($p = 0.61$; Fig. 2C). Note that the present study used only one sham condition as a control for the high intensity rhythmic condition.

We performed additional analyses on the right parieto-occipital electrodes and found the same pattern of findings. There were no statistically significant differences with any intensity conditions and protocols (all p-values > 0.05), except at the medium intensity, arrhythmic condition ($t_{15} = -4.01$, $p = 0.023$; Cohen's $d = 0.23$ and $\eta^2 = 0.05$).

Long-term aftereffect

In the following analyses ($n = 16$), we focused on the IAF, because the entrainment hypothesis predicts that the most pronounced effects should occur in frequencies at and close to the IAF (Glass, 2001). We compared the rhythmic and sham protocols in the high intensity condition using a non-parametric cluster-based permutation test of the normalized alpha power. The analysis did not reveal any significant difference between the real and sham groups ($p = 0.30$; Fig. 3).

Next, we compared the rhythmic and arrhythmic protocols using non-parametric cluster-based permutation tests on the normalized alpha power. Again, the test revealed no significant differences between these protocols with any intensity conditions (all p-values > 0.05; see Fig. 4). Similarly, the test revealed no significant differences with any intensities at the right parieto-occipital electrodes (all p-values > 0.05).

These findings indicate that relative to the arrhythmic, control conditions, real rTMS at ca. 20 and 50 $^{mV}/_{mm}$ peak absolute electric field did not change the spectral power in the inter-burst intervals in the individual alpha frequency ± 1 Hz range. There was a non-significant ($p = 0.08$) decrease in alpha power relative to the arrhythmic condition, real rTMS at ca. 35 $^{mV}/_{mm}$ for up to 10 s on the stimulated site.

DISCUSSION

In the present study, we investigated the electrophysiological aftereffects of rhythmic, arrhythmic, and sham rTMS protocols in humans. We defined aftereffects as changes in the alpha power (8–14 Hz) during the inter-burst intervals. We measured short-term aftereffects, i.e. up to two seconds after stimulation, and long-term aftereffects, i.e. from two to ten seconds after stimulation. We expected that rhythmic rTMS would entrain alpha oscillations and lead to increased alpha power after rTMS (Hanslmayr et al., 2014). Based on the entrainment echo hypothesis, we expected alpha power to be increased for up to ca. two seconds after each burst with rhythmic stimulation. We also expected that neither sham nor arrhythmic rTMS would have any aftereffects on power modulation.
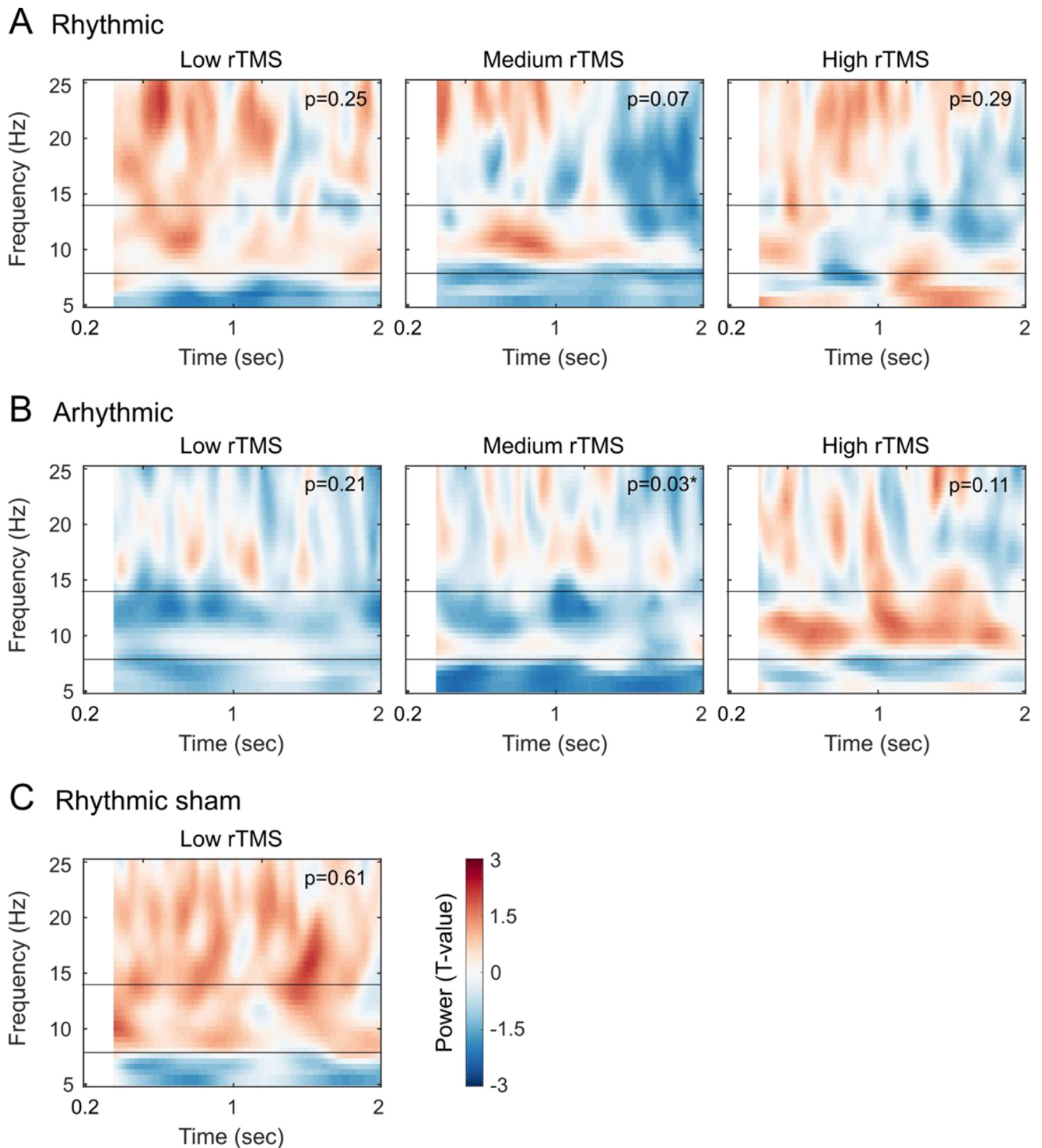
Fig. 2. Alpha power change after the rTMS bursts compared with the baseline time period (activation vs. baseline analysis). Time-frequency plots show the power in the range from 5 to 25 Hz **(A)** in the rhythmic, main, **(B)** in the arrhythmic, control and **(C)** in the sham rTMS protocols. *P*-values are added to each figure to indicate statistical significance. Horizontal lines represent the limits of alpha rhythm (8–14 Hz). Zero on the abscissa corresponds to the time of stimulation offset. Statistical analysis was performed with a gap of 200 ms to reduce the influence of residual TMS artifacts.

Contrary to our expectations, we observed no aftereffects on alpha power in the rhythmic rTMS protocols with all intensities. In the medium intensity condition, we observed a significant decrease in alpha power in the arrhythmic, and a slight, but non-significant increase in the rhythmic protocol. When studying the entire ten-second inter-burst interval, we found no significant differences in alpha power between the
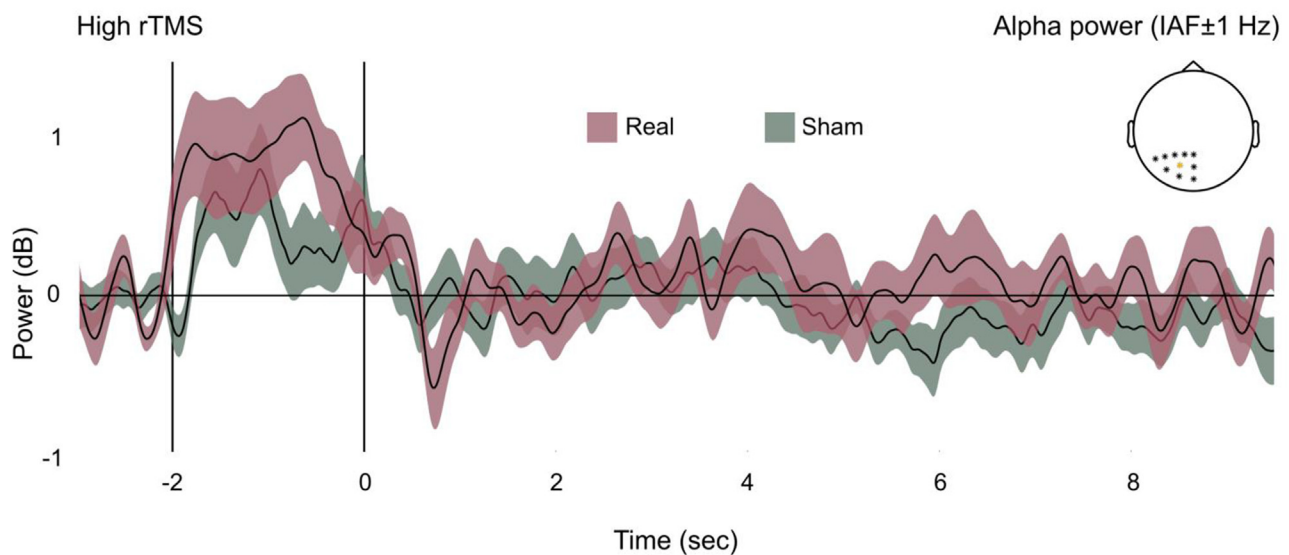
Fig. 3. Real rTMS did not change the spectral power relative to the sham rTMS at the individual alpha frequency. The plots show the mean (black line) and SEM (shaded area) of normalized alpha power during the whole trial. The power at IAF $\pm$ 1 Hz was averaged over ten parietal channels around the stimulation electrode – PO3 (red). The vertical lines at -2 and zero seconds represent stimulation onset and offset, respectively. Note that we aligned the analysis relative to the end of rTMS bursts. Thus, the exact beginning at -2 second varies according to the IAF. (For interpretation of the references to color in this figure legend, the reader is referred to the web version of this article.)

rhythmic and sham or rhythmic and arrhythmic protocols. We found the same pattern of aftereffects at both the stimulated and non-stimulated sites.

Compared to conventional rTMS studies that typically use electric fields of ca. 100 $^{mV}/_{mm}$, the present study applied field strengths that were several times weaker ranging from 20 to 50 $^{mV}/_{mm}$. One might argue that the applied electric field strength was simply too weak to induce any aftereffects. Following the above argument, one should find more robust aftereffects on alpha power in studies using much stronger stimulation intensities and thus greater electric field strengths. To gain a comprehensive overview, we performed a literature search on rTMS studies using conventional intensities published between 1989 and 2017 (see Supplemental Experimental Procedures for details).

In this search, we focused on studies that evaluated the aftereffects of 10 Hz rTMS on alpha power. We identified 16 eligible articles; ten of which described no aftereffects after rTMS. Two articles described an increase, two articles observed both an increase and a decrease, and one article described a decrease. One article reported incomplete statistical tests to support the claimed aftereffect (e.g., post-hoc tests were missing; see Table S1 for more details). One plausible reason for the contradictory findings may be the known variability in the stimulation parameters, such as the number of pulses, duration of the inter-train intervals, the neuronal state of the stimulated area, etc. (Huang et al., 2017).

Moreover, these studies also differ in how they operationalize the rTMS-induced aftereffects. Whereas some studies focused on the short inter-burst intervals (e.g., Puzzo et al., 2013), others analyzed the time interval after the end of the rTMS protocol (e.g., Woźniak-K

waśniewska et al., 2014). Furthermore, studies may also differ in whether they evaluate the aftereffects directly after the end of the rTMS protocol or after a certain delay period (e.g., Weisz et al., 2014). In the present literature search, this delay period varied from several minutes (e.g., Valiulis et al., 2012) up to one week (e.g., Narushima et al., 2010). Finally, these studies recruited healthy persons as well as patients (e.g., medication resistant major depression (Valiulis et al., 2012)), which is an important factor to consider when evaluating the aftereffects of rTMS.

Taken together, it is difficult to draw clear conclusions about the expected direction of the EEG aftereffects following 10 Hz rTMS. Therefore, the result of the literature analysis was that the evidence about the aftereffects on spectral power in conventional rTMS studies is currently inconclusive.

At conventional intensities, 10 Hz rTMS is supposed to increase the corticospinal excitability level (Huang et al., 2017). The most typical outcome measure in humans is the peak-to-peak amplitude of the single pulse TMS-induced motor evoked potential. Many studies have found increased motor evoked potential amplitudes after the end of a 10 Hz rTMS protocol that lasted for a few minutes (Arai et al., 2007).

Inhibitory synaptic effects likely play a significant role in the pattern of aftereffects. For instance, a previous *in vitro* tissue culture study provided evidence that 10 Hz repetitive magnetic stimulation induced long-term depression in inhibitory synapses (Lenz et al., 2016). Moreover, scalp EEG alpha oscillations have been associated with cortical inhibition in humans (Klimesch et al., 2007). Therefore, future studies should also investigate the aftereffects of 10 Hz rTMS on the corticospinal
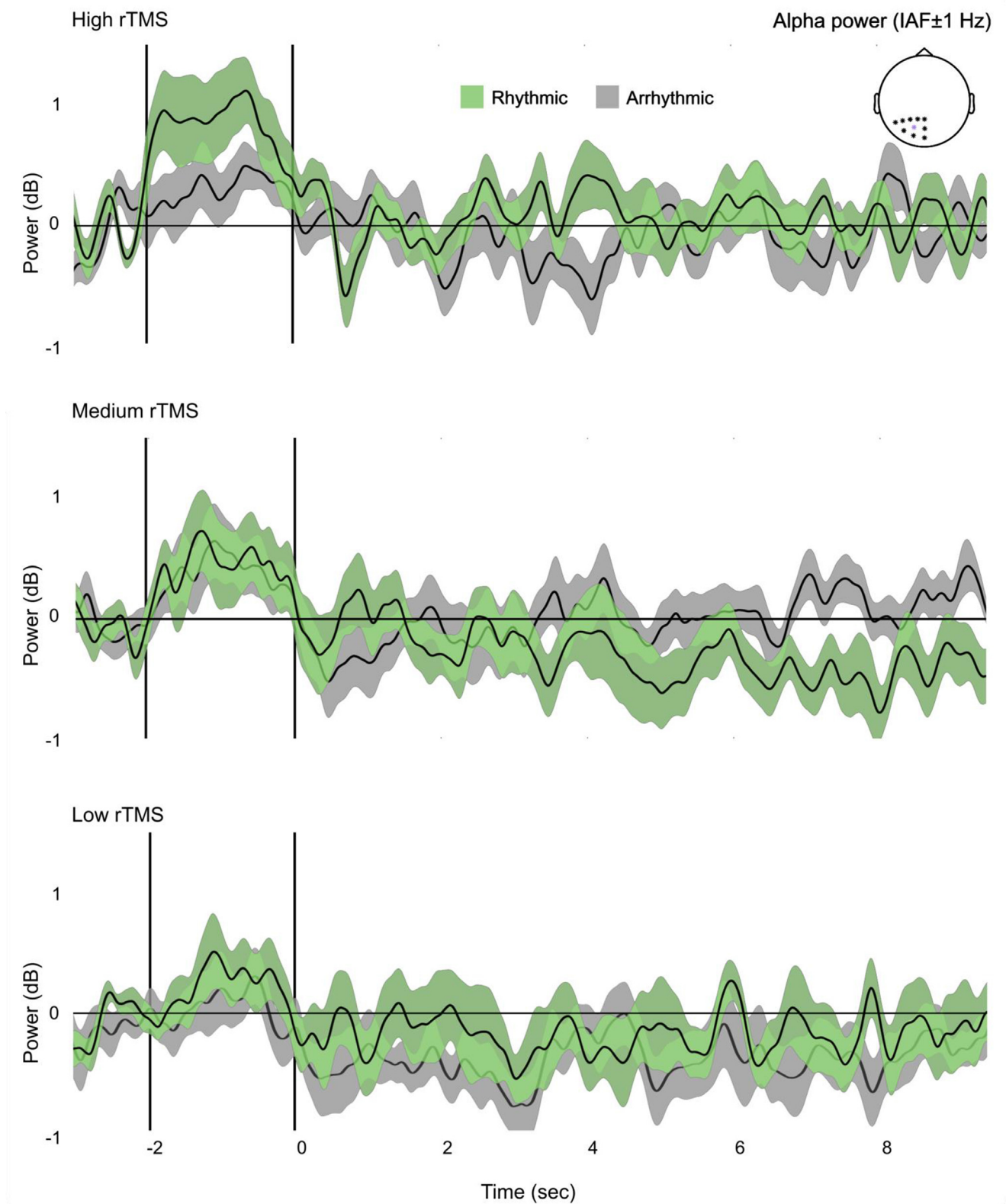
Fig. 4. Lack of significant differences in the individual alpha power between rhythmic and arrhythmic rTMS. The plots show the mean (black line) and SEM (shaded area) of alpha power after rTMS bursts (time = 0). The power is normalized to the 1-second-long baseline period directly before the rTMS bursts with decibel correction and averaged over groups and ten parietal channels. Alpha power is extracted at IAF ± 1 Hz. Statistical analysis showed no significant difference between the rhythmic and arrhythmic conditions for any stimulation intensity. The vertical lines at −2 and zero seconds represent stimulation onset and offset, respectively. Note that we aligned the analysis relative to the end of rTMS bursts. Thus, the exact beginning at −2 s varies according to the IAF.

excitability level together with the EEG changes when applying weak electric fields, such as in the present study.

In the present study, we focused on electrophysiological aftereffect recorded during the inter-burst intervals. At medium intensities (ca. 35 $^{mV}/_{mm}$), arrhythmic rTMS significantly reduced the alpha power shortly after the rTMS bursts, while the increase in alpha power after rhythmic rTMS was not statistically significant. These findings may be explained by previous observations that cortical inhibitory mechanisms might have lower intensity thresholds than those producing excitation (Moliadze et al., 2012). We speculate that the arrhythmic recruitment of inhibitory synapses may have interfered with the spike-timing dependent plasticity and hence decreased neural synchrony and alpha power in the inter-burst intervals. It remains to be seen which electric field intensities can induce more robust and long-term aftereffects that are manifest for up to several minutes or even longer after the end of the protocol. Future studies should preferably deliver rhythmic and arrhythmic protocols in separate sessions. This study design may facilitate studying the individual contribution of each protocol type in other forms of plasticity, including meta-plasticity and, homeostatic plasticity.

CONFLICT OF INTEREST

The authors declare no conflict of interest.

AUTHORS CONTRIBUTION

Authors contribution was prepared according to the Contributor Roles Taxonomy. Conceptualization: ZT; Study design: EZ, MM, ZT and WP; Formal analysis: EZ; Funding acquisition: ZT, WP; Investigation: EZ and ZT; Methodology: EZ and ZT; Project administration: EZ, ZT and WP; Software: EZ and ZT; Supervision: MM and WP; Visualization: EZ and ZT; Writing - original draft: EZ and ZT with the critical contribution of all authors.

ACKNOWLEDGEMENTS

REFERENCES

Albouy P, Weiss A, Baillet S, Zatorre RJ (2017) Selective entrainment of theta oscillations in the dorsal stream causally enhances auditory working memory performance. Neuron 94(1):193–206. e5. https://doi.org/10.1016/j.neuron.2017.03.015.

Anastassiou CA, Perin R, Markram H, Koch C (2011) Ephaptic coupling of cortical neurons. Nat Neurosci 14(2):217–223. https://doi.org/10.1038/nn.2727.

Arai N, Okabe S, Furubayashi T, Mochizuki H, Iwata NK, Hanajima R, Terao Y, Ugawa Y (2007) Differences in after-effect between monophasic and biphasic high-frequency rTMS of the human motor cortex. Clin Neurophysiol 118(10):2227–2233. https://doi.org/10.1016/j.clinph.2007.07.006.

Glass L (2001) Synchronization and rhythmic processes in physiology. Nature 410(6825):277–284.

Haegens S, Cousijn H, Wallis G, Harrison PJ, Nobre AC (2014) Inter- and intra-individual variability in alpha peak frequency. NeuroImage 92:46–55. https://doi.org/10.1016/j.neuroimage.2014.01.049.

Hanslmayr S, Matuschek J, Fellner MC (2014) Entrainment of prefrontal beta oscillations induces an endogenous echo and impairs memory formation. Curr Biol 24(8):904–909. https://doi.org/10.1016/j.cub.2014.03.007.

Huang Y-Z, Lu M-K, Antal A, Classen J, Nitsche M, Ziemann U, Ridding M, Hamada M, Ugawa Y, Jaberzadeh S, Suppa A, Paulus W, Rothwell J (2017) Plasticity induced by non-invasive transcranial brain stimulation: a position paper. Clin Neurophysiol 128(11):2318–2329. https://doi.org/10.1016/j.clinph.2017.09.007.

Ilmoniemi RJ, Hernandez-Pavon JC, Makela NN, Metsomaa J, Mutanen TP, Stenroos M, Sarvas J (2015) Dealing with artifacts in TMS-evoked EEG. In: Proceedings of the Annual International Conference of the IEEE Engineering in Medicine and Biology Society. p. 230–233. https://doi.org/10.1109/EMBC.2015.7318342.

Klimesch W, Sauseng P, Hanslmayr S (2007) EEG alpha oscillations: the inhibition-timing hypothesis. Brain Res Rev 53(1):63–88. https://doi.org/10.1016/j.brainresrev.2006.06.003.

Lenz M, Galanis C, Müller-Dahlhaus F, Opitz A, Wierenga CJ, Szabó G, Ziemann U, Deller T, Funke K, Vlachos A (2016) Repetitive magnetic stimulation induces plasticity of inhibitory synapses. Nat Commun 7(1). https://doi.org/10.1038/ncomms10020.

Lenz M, Vlachos A (2016) Releasing the cortical brake by non-invasive electromagnetic stimulation? rTMS induces LTD of GABAergic neurotransmission. Front Neural Circuits 10:96. https://doi.org/10.3389/fncir.2016.00096.

Moliadze V, Atalay D, Antal A, Paulus W (2012) Close to threshold transcranial electrical stimulation preferentially activates inhibitory networks before switching to excitation with higher intensities. Brain Stimulation 5(4):505–511. https://doi.org/10.1016/j.brs.2011.11.004.

Narushima K, McCormick LM, Yamada T, Thatcher RW, Robinson RG (2010) Subgenual cingulate theta activity predicts treatment response of repetitive transcranial magnetic stimulation in participants with vascular depression. J Neuropsychiatry Clin Neurosci 22(1):75–84.

Oldfield RC (1971) The assessment and analysis of handedness: The Edinburgh inventory. Neuropsychologia 9(1):97–113. https://doi.org/10.1016/0028-3932(71)90067-4.

Opitz A, Windhoff M, Heidemann RM, Turner R, Thielscher A (2011) How the brain tissue shapes the electric field induced by transcranial magnetic stimulation. NeuroImage 58(3):849–859. https://doi.org/10.1016/j.neuroimage.2011.06.069.

Paulus W, Peterchev AV, Ridding M (2013) Transcranial electric and magnetic stimulation: technique and paradigms. Handbook Clin Neurol 116:329–342.

Puzzo I, Cooper NR, Cantarella S, Fitzgerald PB, Russo R (2013) The effect of rTMS over the inferior parietal lobule on EEG sensorimotor reactivity differs according to self-reported traits of autism in typically developing individuals $. Brain Res 1541:33–41. https://doi.org/10.1016/j.brainres.2013.10.016.

Romei V, Thut G, Mok RM, Schyns PG, Driver J (2012) Causal implication by rhythmic transcranial magnetic stimulation of alpha frequency in feature-based local vs. global attention. Eur J Neurosci 35:968–974. https://doi.org/10.1111/j.1460-9568.2012.08020.x.

Thielscher A, Antunes A, Saturnino GB (2015) Field modeling for transcranial magnetic stimulation: a useful tool to understand the physiological effects of TMS? In: Proceedings of the Annual International Conference of the IEEE Engineering in Medicine and Biology Society. p. 222–225. https://doi.org/10.1109/EMBC.2015.7318340.

Thut G, Schyns PG, Gross J (2011) Entrainment of perceptually relevant brain oscillations by non - invasive rhythmic stimulation of

the human brain. Front Psychol 2:170. https://doi.org/10.3389/fpsyg.2011.00170.

Valiulis V, Gerulskis G, Dapšys K, Vištartaitė G, Šiurkutė A (2012) Electrophysiological differences between high and low frequency rTMS protocols in depression treatment. Acta Neurobiol Exp 72 (3):283–295.

Weisz N, Lüchinger C, Thut G, Müller N (2014) Effects of individual alpha rTMS applied to the auditory cortex and its implications for the treatment of chronic tinnitus. Hum Brain Mapp 35(1):14–29. https://doi.org/10.1002/hbm.22152.

Woźniak-Kwaśniewska A, Szekely D, Aussedat P, Bougerol T, David O (2014) Changes of oscillatory brain activity induced by repetitive transcranial magnetic stimulation of the left dorsolateral prefrontal cortex in healthy subjects. NeuroImage 88:91–99. https://doi.org/10.1016/j.neuroimage.2013.11.029.

Wu W, Keller CJ, Rogasch NC, Longwell P, Shpigel E, Rolle CE, Etkin A (2018) ARTIST: A fully automated artifact rejection algorithm for single-pulse TMS-EEG data. Hum Brain Mapp 39 (4):1607–1625. https://doi.org/10.1002/hbm.v39.410.1002/hbm.23938.

Zmeykina E, Mittner M, Paulus W, Turi Z (2020) Weak rTMS-induced electric fields produce neural entrainment in humans. Sci Rep 10 (1):1–16. https://doi.org/10.1038/s41598-020-68687-8.

APPENDIX A. SUPPLEMENTARY DATA

Supplementary data to this article can be found online at https://doi.org/10.1016/j.neuroscience.2021.04.027.